



# Single-Molecule Analysis of the Recognition Forces Underlying Nucleo-Cytoplasmic Transport\*\*

Martina Rangl, Andreas Ebner, Justin Yamada, Christian Rankl, Robert Tampé, Hermann J. Gruber, Michael Rexach,\* and Peter Hinterdorfer\*

Macromolecular transport between the cell nucleus and cytoplasm is gated by the nuclear pore complex (NPC). The NPC<sup>[1]</sup> is a 65–125 MDa ring structure that spans the nuclear envelope<sup>[2]</sup> (Figure 1). It has 30 distinct proteins or nucleoporins (nups) in multiple copies totaling about 400–500 nups per NPC.<sup>[3,4]</sup> Based on hydrophobicity and size,<sup>[5–7]</sup> it gates nucleocytoplasmic traffic of macromolecules greater than 30 kDa or about 3 nm in diameter, including most nuclear proteins and ribonucleoproteins.<sup>[8]</sup> Those shuttling cargos expose transport signals (i.e. short AA sequences) that are selectively captured by shuttling karyopherins (kaps),<sup>[9]</sup> to gain passage across the NPC. For this, the kaps continuously permeate the NPC gate by interacting with so-called FG nups thereby escorting molecules of different shapes and sizes across the barrier.<sup>[10]</sup>

Approximately one third of nups (about 150) in the NPC feature phenylalanine–glycine repeats in intrinsically disordered domains (FG nups)<sup>[11]</sup> that operate to form the NPC permeability barrier,<sup>[5,12]</sup> whereas the other nups are forming the NPC scaffold. These line the periphery and the interior of the NPC transport conduit,<sup>[12,13]</sup> exposing thousands of FG repeats that serve as ligands for kaps for chaperoning cargoes through the NPC pore.<sup>[14–16]</sup> The arrangement of disordered FG nups within the NPC (the barrier architecture) and the mechanism(s) by which kaps permeate the barrier are unresolved.

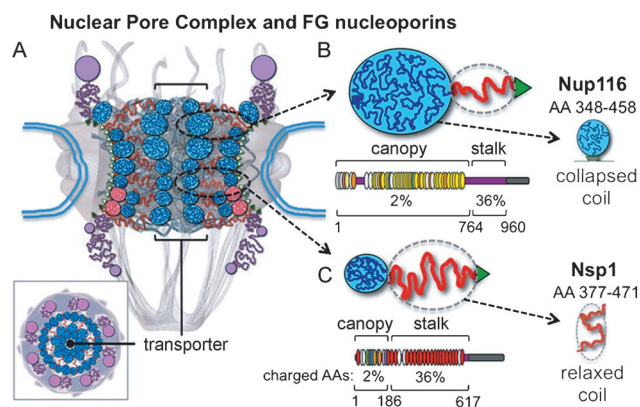


**Figure 1.** Diagrams of the NPC and its disordered FG nups. A) Cross-section featuring the NPC ring-scaffold (center), cytoplasmic fibers (top), and nuclear basket (bottom). Intrinsically disordered FG nups are outlined in blue (collapsed coils) and red (extended coils) lines forming the transporter/plug gate structure in the NPC channel.<sup>[11]</sup> A top view is also shown (bottom left). B) The *S. cerevisiae* FG nups Nup116. As a representative of “cohesive” nups it primarily adopts collapsed coil/“canopy” configurations (blue line, globule). Below FG repeats are shown as thin ovals (GLFG in yellow; FxFG in red) and the amount of charged AA is indicated. The portion of Nup116’s canopy (AA 348–458) is highlighted. C) Nsp1 as a representative of “repulsive” nups. It adopts a relaxed-to-extended “stalk” region (red line) and it has a high content of charged AAs and features mainly FxFG motifs (bottom). The portion of Nsp1’s stalk (AA 377–471) is highlighted.

[\*] Dr. M. Rangl, Prof. A. Ebner, Prof. H. J. Gruber, Prof. P. Hinterdorfer  
Institute for Biophysics, Johannes Kepler University Linz  
Gruberstr. 40, 4020 Linz (Austria)  
E-mail: peter.hinterdorfer@jku.at

J. Yamada, Prof. M. Rexach  
Department of Molecular, Cell and Developmental Biology, Sin-  
sheimer Laboratories, University of California  
Santa Cruz, CA 95064 (USA)  
E-mail: mrexach@ucsc.edu

Dr. C. Rankl  
Agilent Technologies Austria GmbH  
Mooslackengasse 17, 1190 Wien (Austria)

Prof. R. Tampé  
Institute of Biochemistry, Biocenter  
Goethe-University Frankfurt, Frankfurt (Germany)

[\*\*] This work was supported by NIH (RO1 grant number GM077520 to M.R.), the Austrian Science Fund (grant number FWF W1201 N13 to P.H.), L’Oréal Austria Scholarship “For Women in Science” to P.H., Johannes Kepler University Scholarship for young scientists to P.H., and Austrian FFG-MNT-ERA.NET Project IntelliTip (grant number 823980 to A.E.).

Supporting information for this article is available on the WWW under <http://dx.doi.org/10.1002/anie.201305359>.

All current models of NPC structure and function propose that interactions between kaps and nup FG repeats govern the translocation process,<sup>[3,13,17,18]</sup> and that the energetics of binding are coupled to translocation since chemical energy is not consumed.<sup>[8]</sup> Two of the models<sup>[13,17]</sup> further suggest that hydrophobic interactions between FG nups themselves are key element in the gating mechanism. Hence, it is of key interest to quantify the interaction forces between nup FG repeats, and how they compare to the binding forces between kap and nup FG repeats.

We thus directly probed the force of interaction and the molecular dissociation rate between nup FG repeats and between kap and FG repeats using molecular recognition force spectroscopy (MRFS). MRFS measures intermolecular interaction forces between single molecules.<sup>[19,20]</sup> It was previously used to characterize FG motif binding sites on importin (a particular kap) and their modulation by Ran-induced conformational changes by which transport direction, cargo release, and recycling of kaps are regulated.<sup>[21]</sup> Also, by studying the interaction of importin with Ran, 1) alternative conformational states in the complex were observed,<sup>[22]</sup>

2) different modes of protein activation were discriminated,<sup>[23]</sup> and 3) the interaction energy landscape roughness was determined.<sup>[24]</sup> Last, an exploration of the nanomechanical properties of nup FG domains by MRFS led to the hypothesis that importins reversibly collapse FG domains into compact structures (thereby opening space through the permeability barrier) by capturing multiple FG repeats simultaneously.<sup>[25]</sup>

Within this study we performed MRFS experiments (Figure 2) to measure interaction forces, stoichiometry, and

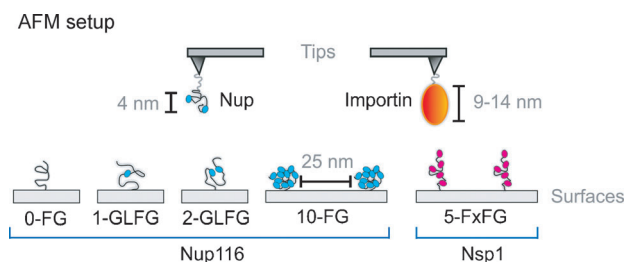


**Figure 2.** Diagram of the MRFS experimental approach. A single nup or importin molecule was immobilized at the apex of an AFM tip using a flexible 6 nm long linker (Figure S2). FG domains were immobilized on flat mica surfaces (average distance of about 25 nm) using the same coupling chemistry.

molecular dissociation rates between nup FG repeats; and between importin and two distinct categories of FG domains: collapsed coils featuring a low content of charged AAs, GLFG repeats, and a “cohesive” nature (they stick to each other); and relaxed-to-extended coils featuring FxFG repeats, a high content of charged AAs, and a “repulsive” nature (they repel all FG domains).<sup>[5,13]</sup> Portions of *S. cerevisiae* Nup116 and Nsp1 FG domains, and human importin beta, were used as representatives.<sup>[13,15,21,26–28]</sup> The Nup116 FG domain (AA 348–458) is a 110 AA collapsed coil (see Figure S1 in the Supporting Information), adopts about 4 nm diameter globular configurations at 30 °C ( $R_s = 20.4 \text{ \AA}$ ), has a 3 % charged-AA content, and features ten FG motifs.<sup>[13]</sup> The Nsp1 FG domain (AA 377–471) is a 95 AA relaxed coil (Figure S1) with a dynamic backbone that fluctuates widely in hydrodynamic dimensions.<sup>[13]</sup> It has a 5.4 nm average diameter ( $R_s = 26.8 \text{ \AA}$ ), a 34 % charged-AA content, and features five FxFG repeats. Variants of Nup116 were constructed by FG > AG substitutions to contain zero (0-FG Nup116), one (1-GLFG Nup116), or two (2-GLFG Nup116) FG repeats instead of ten (10-FG Nup116; Figure 2 and Figure S1). The elimination of phenylalanines shifted their structure to more dynamic configurations<sup>[13]</sup> because of a loss of intramolecular interactions.<sup>[26]</sup>

The interaction force between nup FG repeats was measured using functionalized sensor tips and surfaces (Figure 2, Figures S2 and S3) and recording force–distance cycles (Figure S4). The 0-FG Nup116 on the tip and mica surfaces produced only negligible interactions (Figure 3A). In contrast, the 1-GLFG Nup116 molecules formed single bonds, and the 2-GLFG Nup116 molecules formed single (not included) and double bonds with dissociation forces of about 25 pN and 50 pN, respectively (Figure 3A). This was

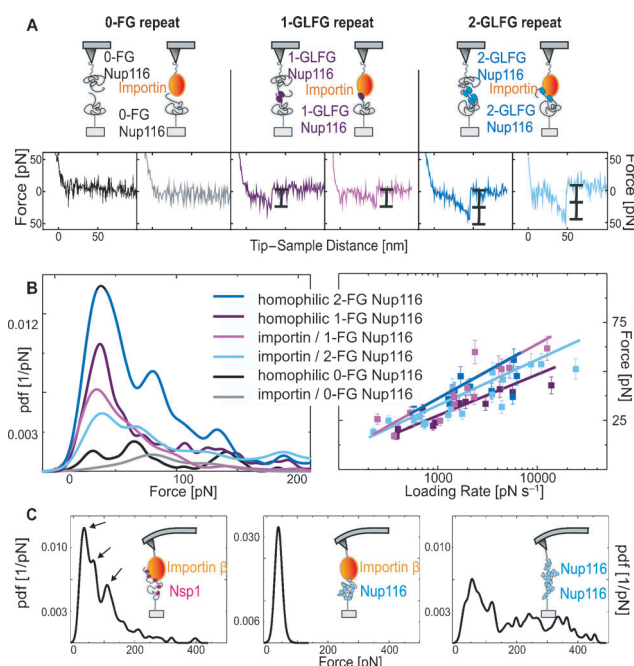


**Figure 3.** MRFS analysis of nup–nup and importin–nup interactions. A) MRFS analysis of homophilic Nup116 interactions and importin/Nup116 interactions. Homophilic 0-FG Nup116 interactions and importin/0-FG Nup116 interactions (left) showed negligible binding. Homophilic 1-GLFG Nup116 interactions and importin/1-GLFG Nup116 interactions (center) showed a single unbinding event (black bracket). Homophilic 2-GLFG Nup116 interactions and importin/2-GLFG Nup116 interactions showed two unbinding events: double-force events (right) and single-force events (not included). B) Pdf analysis of MRFS measurements from nup–nup and importin–nup interactions. Interactions involving FG domains with zero, one, and two GLFG repeats showed zero, one, and two force maxima, respectively (left panel). Loading rate dependencies of the first force peak (right panel) yielding the kinetic off-rates and the distances of energy minimum (bound state) to maximum (unbound state) in the energy landscape (Table 1, Figure S5). C) Pdf analysis of MRFS measurements from importin–nup interactions. Importin on the tip and 5-FxFG Nsp1 (left) or 10-FG Nup116 (center) on mica. Importin/5-FxFG Nsp1 complexes produced single-, double-, and triple-force unbinding events (arrows), whereas importin/10-FG Nup116 showed only single unbinding events. Homophilic 10-FG Nup116 interactions (right) showed multiple unbinding events and a broad force distribution.

confirmed using statistical analyses that combined more than 200 force values for each experimental configuration to construct experimental probability density functions (pdfs) of interaction forces (Figure 3B). Single interactions (as the homophilic 1-GLFG Nup116 interaction) resulted in one significant peak and double simultaneous interactions (as the homophilic 2-GLFG Nup116 interaction) in two discrete peaks. Homophilic 0-FG Nup116 interactions produced only low background signals with no distinguishable peak(s). Last, homophilic 10-FG Nup116 interactions showed broad force distributions, consistent with numerous FG repeat interactions (Figure 3C, right).

Importin/FG nup interactions were also analyzed. The 0-FG Nup116 domain produced no interactions with importin (Figure 3A, left), and only background signals in the force distribution analyses (Figure 3B). In contrast, the 1-GLFG

Nup116 molecules showed one interaction with importin, and the 2-GLFG Nup116 showed two interactions (Figure 3 A). Consistently, the force distributions resulted in one and two significant peaks for the interactions, respectively (Figure 3 B). Their force quanta were comparable to the ones from homophilic nup FG interactions (Figure 3 B). Lastly, the 5-FxFG Nsp1 molecule achieved three distinct binding events corresponding to single, double, and triple interactions; these were confirmed as separate peaks in the force pdf distributions (Figure 3 C, left). Hence, at least three FxFG repeats (or two GLFG repeats; see above) could be captured simultaneously by importin. Next we tested whether importin binds collapsed-coil FG domains, such as 10-FG Nup116, similarly to relaxed-coil FG domains. Surprisingly, importin captured only one of ten FG repeats simultaneously, as evident from a single maximum in the force pdf profile (Figure 3 C, center). Only one of ten FG repeats in the collapsed-coil Nup116 FG domain appeared available for importin binding at any given moment. Hence, intramolecular FG repeat interactions in collapsed coil FG domains may dominate over interactions with importin, suggesting that importins are guided to follow paths between FG domain globules across the NPC, as proposed.<sup>[13,26]</sup>

Variations in the loading rate ( $r$ ) during MRFS experiments (Figure 3 B and Figure S5) allowed an estimation of kinetic off-rate constants ( $k_{\text{off}}$ ) and energy barrier distances ( $x_{\beta}$ ) for the interactions (Table 1).<sup>[29,30]</sup> Interactions involving

**Table 1:** Kinetic parameters of nup–nup and importin–nup interactions.  $k_{\text{off}}$  is the kinetic off-rate constant;  $x_{\beta}$  is the energy barrier distance.

Interactions	$k_{\text{off}}$ [ $\text{s}^{-1}$ ]	$x_{\beta}$ [ $\text{\AA}$ ]
homophilic 1-GLFG Nup116	$5.41 \pm 3.56$	$4.52 \pm 1.29$
homophilic 2-GLFG Nup116	$4.26 \pm 5.86$	$3.36 \pm 1.88$
importin with 1-GLFG Nup116	$4.23 \pm 1.79$	$3.39 \pm 0.64$
importin with 2-GLFG Nup116	$3.99 \pm 2.18$	$4.05 \pm 0.79$
importin with 10-FG Nup116	$4.87 \pm 1.01$	$1.14 \pm 0.20$
importin with 5-FxFG Nsp1	5.81	1.49

a single FG repeat binding to importin, or to another nup FG repeat, showed comparable off-rates with 4–5 dissociations per second or about 200 ms bond lifetimes (Table 1). This was forty-times slower than the recorded interaction time of importin with an NPC during transit (3–7 ms).<sup>[31]</sup> Hence, a particular mechanism like Ran-GTP triggered cargo dissociation from importin, environmental factors such as nup location, and local molecule density variations previously reported as “highway” effect must accelerate FG repeat dissociations.<sup>[32]</sup> In the latter, kap translocation occurs on different “lanes” depending on their concentration and, kap crowding is a key element in fast transport rates at the center of the pore.

The  $k_{\text{off}}$  and  $x_{\beta}$  values were comparable among the single interactions of importin with Nup116 and Nsp1 FG domains (Table 1), despite these nups featuring different types of FG motifs, AA composition, and categories of disordered structure (Figure S1). Hence, all interactions appeared dominated by the common phenylalanine in the FG repeats, and not by

intervening AA sequences. This was unexpected for the homophilic interactions because amyloid-like bonds involving residues between FG motifs have been reported.<sup>[33]</sup> However, such interactions require minutes to hours of incubation to form,<sup>[34]</sup> clearly beyond the timescale explored here.

In conclusion, the force distributions and loading rate dependencies (Table 1) for single nup–nup and importin–nup interactions were energetically equivalent. This key finding supports the hypothesis that importins enter and diffuse across the NPC by substituting FG repeat interactions of nups with energetically equivalent importin–FG repeat interactions. In addition, the different interaction behavior of collapsed and extended coils with importin endorse the assumption of distinct pathways within the transport channel.

Received: June 21, 2013

Published online: September 5, 2013

**Keywords:** atomic force spectroscopy · membranes · nuclear pore complexes · nucleoporins · recognition

- [1] C. M. Feldherr, E. Kallenbach, N. Schultz, *J. Cell Biol.* **1984**, *99*, 2216–2222.
- [2] A. Hoelz, E. Debler, G. Blobel, *Annu. Rev. Biochem.* **2011**, *80*, 613–643.
- [3] M. P. Rout, J. D. Aitchison, A. Suprpto, K. Hjertaas, Y. Zhao, B. T. Chait, *J. Cell Biol.* **2000**, *148*, 635–651.
- [4] J. M. Cronshaw, A. N. Krutchinsky, W. Zhang, B. T. Chait, M. J. Matunis, *J. Cell Biol.* **2002**, *158*, 915–927.
- [5] S. S. Patel, B. Belmont, J. Sante, M. Rexach, *Cell* **2007**, *129*, 83–96.
- [6] B. Naim, D. Zbaida, S. Dagan, R. Kapon, Z. Reich, *EMBO J.* **2009**, *28*, 2697–2705.
- [7] K. Ribbeck, D. Gorlich, *EMBO J.* **2002**, *21*, 2664–2671.
- [8] D. Görlich, U. Kutay, *Annu. Rev. Cell Dev. Biol.* **1999**, *15*, 607–660.
- [9] Y. Chook, K. Suël, *Biochim. Biophys. Acta* **2010**, E pub ahead of print.
- [10] S. Wente, M. Rout, *Cold Spring Harbor Perspect. Biol.* **2010**, *2*, p. a000562. Epub.
- [11] D. P. Denning, S. S. Patel, V. Uversky, A. L. Fink, M. Rexach, *Proc. Natl. Acad. Sci. USA* **2003**, *100*, 2450–2455.
- [12] F. Alber et al., *Nature* **2007**, *450*, 695–701.
- [13] J. Yamada et al., *Mol. Cell. Proteomics* **2010**, *9*, 2205–2224.
- [14] A. Radu, M. Moore, G. Blobel, *Cell* **1995**, *81*, 215–222.
- [15] R. Bayliss, T. Littlewood, L. A. Strawn, S. R. Wente, M. Stewart, *J. Biol. Chem.* **2002**, *277*, 50597–50606.
- [16] D. Denning, M. Rexach, *Mol. Cell. Proteomics* **2007**, *6*, 272–282.
- [17] K. Ribbeck, D. Gorlich, *EMBO J.* **2001**, *20*, 1320–1330.
- [18] R. Peters, *Traffic* **2005**, *6*, 421–427.
- [19] E. L. Florin, V. T. Moy, H. E. Gaub, *Science* **1994**, *264*, 415–417.
- [20] P. Hinterdorfer, W. Baumgartner, H. J. Gruber, K. Schilcher, H. Schindler, *Proc. Natl. Acad. Sci. USA* **1996**, *93*, 3477.
- [21] S. Otsuka, S. Iwasaka, Y. Yoneda, K. Takeyasu, S. Yoshimura, *Proc. Natl. Acad. Sci. USA* **2008**, *105*, 16101–16106.
- [22] R. Nevo, C. Stroh, F. Kienberger, D. Kaftan, V. Brumfeld, M. Elbaum, Z. Reich, P. Hinterdorfer, *Nat. Struct. Biol.* **2003**, *10*, 553–557.
- [23] R. Nevo, V. Brumfeld, M. Elbaum, P. Hinterdorfer, Z. Reich, *Biophys. J.* **2004**, *87*, 4, 2630–2634.
- [24] R. Nevo, V. Brumfeld, R. Kapon, P. Hinterdorfer, Z. Reich, *EMBO Rep.* **2005**, *6*, 482–486.

- [25] R. Y. Lim, B. Fahrenkrog, J. Köser, K. Schwarz-Herion, J. Deng, U. Aebi, *Science* **2007**, *318*, 640–643.
  - [26] V. Krishnan, E. Lau, J. Yamada, D. Denning, S. Patel, M. Colvin, M. Rexach, *PLoS Comput. Biol.* **2008**, *4*, e1000145.
  - [27] T. A. Isgro, K. Schulten, *Structure* **2005**, *13*, 1869–1879.
  - [28] C. Müller, G. Cingolani, C. Petosa, K. Weis, *Nature* **1999**, *399*, 221–229.
  - [29] E. Evans, K. Ritchie, *Biophys. J.* **1997**, *72*, 1541–1555.
  - [30] C. Rankl, F. Kienberger, L. Wildling, J. Wruss, H. J. Gruber, D. Blaas, P. Hinterdorfer, *Proc. Natl. Acad. Sci. USA* **2008**, *105*, 17778–17783.
  - [31] W. Yang, S. Musser, *J. Cell Biol.* **2006**, *174*, 951–961.
  - [32] R. L. Schoch, L. E. Kapinos, R. Y. Lim, *Proc. Natl. Acad. Sci. USA* **2012**, *109*, 16911–16916.
  - [33] C. Ader, S. Frey, W. Maas, H. Schmidt, D. Gorlich, M. Baldus, *Proc. Natl. Acad. Sci. USA* **2010**, *107*, 6281–6285.
  - [34] S. Alberti, R. Halfmann, O. King, A. Kapila, S. Lindquist, *Cell* **2009**, *137*, 146–158.
-